

# Evidence for the Freezing of Supercooled Water by Means of Neutron Irradiation

Matthew Szydalis,\* Yujia Huang, Alvine C. Kamaha, Corwin C. Knight, Cecilia Levy, and Gregory R.C. Rischbieter

*The University at Albany, SUNY*

*Department of Physics*

*1400 Washington Avenue*

*Albany, NY USA 12222-0100*

(Dated: July 16, 2020)

The cloud and bubble chambers have historically been used for particle detection, capitalizing on supersaturation and superheating respectively. Here we present the “snowball chamber,” which utilizes supercooled liquid. In our prototype, an incoming particle triggers crystallization of purified water. We demonstrate water is supercooled for a significantly shorter time with respect to control data in the presence of neutron sources, at a level of  $3-5\sigma$  for  $^{252}\text{Cf}$ , but not a  $^{137}\text{Cs}$   $\gamma$ -ray source. We discuss the possible implications of using this new technology for low-mass dark matter searches.

**PACS numbers:** 95.35.+d, 29.40.V, 29.40.-n, 25.40.Dn

**Keywords:** sub-GeV WIMPs, dark matter direct detection, supercooled water, neutron irradiation

## I. INTRODUCTION

The nature of dark matter has remained an enduring enigma for over eight decades now, for both cosmology and astroparticle physics. A continued lack of unambiguous evidence from a direct detection experiment of the traditional and well-motivated Weakly Interacting Massive Particle (WIMP) has led to a major thrust to consider particle masses both higher and lower than before [1]. The main goal of our work is the development of inexpensive, scalable detectors for low-mass dark matter, using supercooled water. Auxiliary purposes include better neutron and neutrino detection [2].

Water has the advantages of containing hydrogen, ideal for considering dark matter candidates  $O(0.5-1)$  GeV/ $c^2$  in mass due to the recoil kinematics, and the possibility of a high degree of purification on large scales [3]. Threshold detectors with metastable fluid targets are advantageous in dark matter experiments due to their high degree of insensitivity to gamma backgrounds, as demonstrated by bubble chamber experiments such as COUPP [4] and PICO [5]. These detectors rely on depositing enough energy within a critical distance to trigger a phase transition, quantified by the differential energy deposition  $dE/dx$  crossing some threshold. By controlling temperature  $T$  and pressure  $P$ , the recoil energy threshold remains low while maintaining a high  $dE/dx$  threshold.

The motivation for using supercooled water [6] instead of superheated water like in a bubble chamber [7] lies in contrasting the keV-scale energy thresholds achieved in dark matter experiments like PICO which utilize superheating, compared with the lower energy thresholds reported for supercooling, which could bring into reach the lower-mass dark matter frontier. Existing work – especially that of Barahona [8, 9] – is indicative of sub-keV or even sub-eV thresholds at temperatures which are not far from the freezing point, for either the homogeneous or heterogeneous form of nucleation [19].

## II. EXPERIMENTAL SETUP

The concept is shown in Figure 1, and actual experimental setup in Figure 2. A fused quartz tube, ultrasonically cleaned in an ISO3 cleanroom, was prepared with  $22 \pm 1$  grams of water, then fully submerged in a thermoregulation ethanol bath, set over vibration-dampening pads and instrumented with 3 thermocouples for recording the exothermic increase on freezing [10]. These were attached near the top, middle (water line), and bottom (hemisphere). Supplementing the internal thermometers, a fourth one, whose variation had no discernible effect, recorded room temperature. LEDs provided illumination from below, while a borescope provided images.

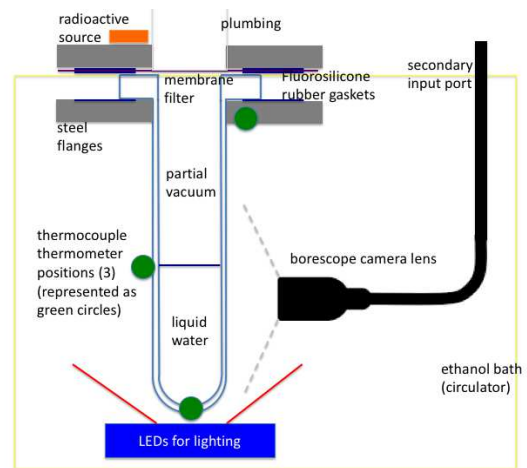


FIG. 1. Diagram of setup, the core of which was a 10-cm-long, cylindrical quartz tube (left) with inner diameter 3.55 cm, outer 4.2 cm, and hemispherical bottom.

Purity is of importance to minimize heterogeneous nucleation. Deionized water was distilled through a 20-nm porous filter membrane into the quartz tube, evacuated via an oil-less pump. The water was cooled in an ethanol bath until it reached a supercooled state, at which point an incident particle could cause the phase transition.

\* Corresponding Author: mszydalis@albany.edu

### III. DATA COLLECTION

The liquid water was continuously cooled at an approximately linear cool-down rate of  $1.90 \pm 0.05$  °C/min. The data were taken both with and without radioactive sources, listed in Table I. AmBe and  $^{252}\text{Cf}$  produce a wide spectrum of neutrons with typical energies  $O(1-10)$  MeV, while the  $^{137}\text{Cs}$  source produced 662 keV  $\gamma$ 's. The "FWBe" was custom-built from a Fiestaware plate [11] and Be foil. Pb was used to block AmBe and Cf  $\gamma$ 's.

Calibration Source	Activity [ $\mu\text{Ci}$ ]	Rate
AmBe ( $\alpha, n$ ) source	90	$\sim 200$ n/s
$^{137}\text{Cs}$ gamma-rays	10	$3.7 \times 10^5$ $\gamma$ /s
FWBe ( $\alpha, n$ ) source	$O(1)$	$O(10)$ n/s
$^{252}\text{Cf}$ fission neutrons	1.0	$\sim 3000$ n/s

TABLE I. Radioactive calibration sources used for this work. Activities are nominal only for neutron sources, as they include all forms of radiation emitted from them. For the case of ( $\alpha, n$ ) sources, there is a low n-yield efficiency, and rates in n/s are separately listed. FW stands for Fiestaware, a ceramic plate rich in uranium nicknamed "radioactive red" [11]. Its activity is estimated. For the AmBe and  $^{252}\text{Cf}$  sources, quoted neutron rates are based upon purchasing identical sources to those used in [12] and [13] respectively.

Control and source runs were interleaved to minimize systematics (48-hour-long runs in 2017; 24 in 2018). Approximately equal numbers of source off vs. on runs were performed, spanning day and night. Beginning at 20 °C, cool-down took 30 minutes. The thermoregulator was set so that the climb to 20 °C was also 30 minutes, to set up the next 1-hour-long cycle.

An increase in temperature was the trigger for recording the images. A 20-sec-long buffer ensured that nucleation was captured, as there was a delay of this order due to thermal transmission (Figure 3). The thermocouple nearest the water line was used, as it reacted soonest.

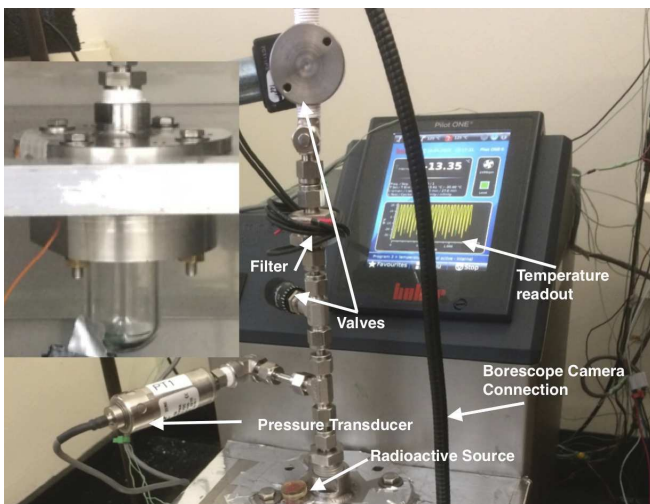


FIG. 2. Photo of actual setup during operation. At left is the quartz tube by itself containing the 22 mL of purified water.

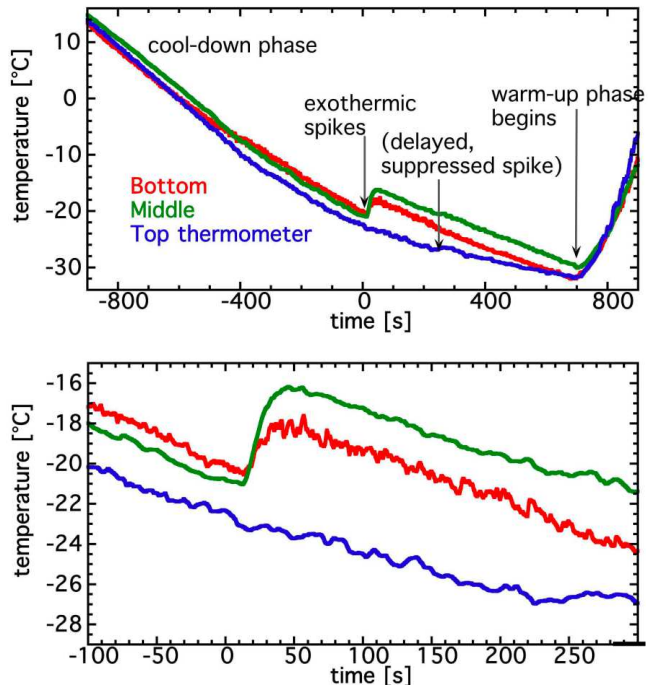


FIG. 3. *Top* The temperature profile for a typical event. The middle and bottom thermometers respond  $12.2 \pm 0.4$  s after the camera indicates freezing (with top responding much later, if at all). Freezing as determined visually is set here as  $t = 0$ . *Bottom* Zoomed-in version near  $t = 0$ .

The use of a thermocouple as trigger is due to low image quality; however, resulting images can nonetheless be informative. In Figure 4, ice crystals scatter LED light more effectively than pure liquid water, revealing nucleation sites against a dark background. This is analogous to the 15 kg COUPP bubble chamber, with lighting orthogonal to camera line of sight [14].

### IV. DATA ANALYSIS

While not the main DAQ trigger, the top thermometer was used to define the supercooled temperature for the purpose of a greater consistency amongst runs, as it was the only one never requiring reattachment.

All data taken were included in the final analysis. Systematic uncertainty in the time spent active, comparable to the statistical uncertainty, is included to address the deviation in control between alternations. All  $T$  measurements have a universal 2.5 °C systematic offset included in values reported here. It was caused by being able to only measure external  $T$ , to avoid nucleation inside. Its value was determined by viewing of the plateau in  $T$  in the top thermocouple during melting, consistently occurring at -2.5 instead of 0 °C.

The nuclear recoil (NR) and electron recoil (ER) rates in the water induced by different sources were simulated using Geant4 (G4) as explained in Section IV B.

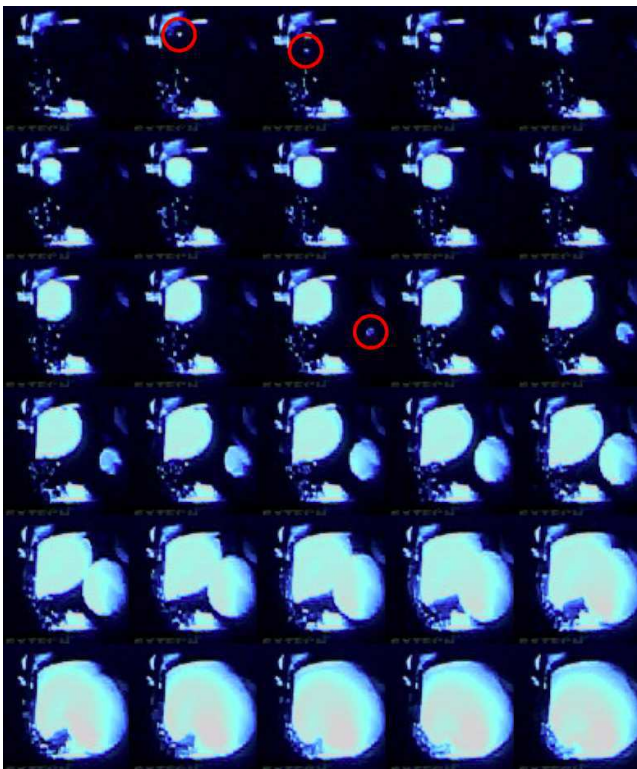


FIG. 4. An example of a triple-nucleation event, from 2018 AmBe data, suspected to be caused by multiple scattering. Red circles indicate the first frames in which a nucleation site appears. The first two “snowballs” merge rapidly; the second appears much later, implying it is from a different neutron. Unlike in a bubble chamber, there is no pressure increase activated after a trigger, so the unfrozen water volume remains active during an ongoing event. Also not like in superheating, nucleation is a slow process here [15]. For brevity, only every 3rd frame is pictured, every 150 ms. This is from unshielded data, but all neutron data sets exhibited a similar behavior.

### A. Results

The main result of this work is that when a  $^{252}\text{Cf}$  neutron source is present water does not remain supercooled as long, on average, over multiple cool-downs, and freezing occurs at higher  $T$ . Figure 5 focuses on Cf; Table II is a concise summary of all data, broken down by individual source, including location on the flange in Figure 2 or side. The difference from control in  $\sigma$  terms is defined using analytic not Gaussian  $\sigma$ . Appendix A contains plots for all sources, and a separate detailed study of AmBe.

Time spent “active” by the water  $\Delta t_{\text{active}}$  is defined as between  $-16^\circ\text{C}$  and freezing. The  $T$  border for determining the definition of active is based on a severe drop-off in trigger rate in every data set, as seen in Fig. 5 bottom. Analyses using  $0^\circ\text{C}$  as the border instead yielded consistent results, including comparable statistical significance. Less time spent supercooled compared to control data implies sensitivity to radiation.

Table II indicates control and  $\gamma$  results are nearly identical (plot in Appendix A) despite a higher ER rate than

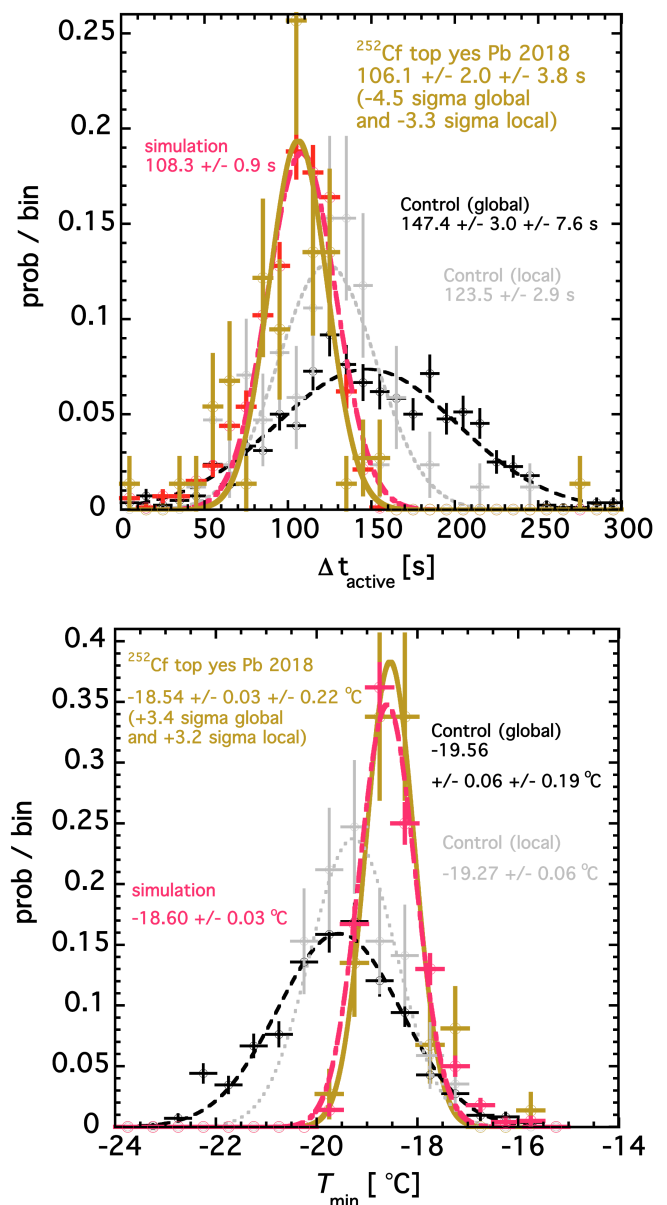


FIG. 5. *Top* Histogram of  $^{252}\text{Cf}$  active time (10 s bins) with Gaussian fits, in gold points and line respectively, compared to control, with black for all data with the same setup, and gray for neighboring control runs only. The latter, local-only comparison is more conservative, and while no longer requiring a systematic error bar, lowers the statistical significance of the disagreement between Cf and control. However, there is no reason not to combine all (2018) control data as done in black. G4 was used to determine energy and  $dE/dx$  distributions, with an additional simulation adding thresholds on top of them and efficiency afterwards, in pink. *Bottom* Same data but looking instead at minimum  $T$  achieved before phase transition, showing consistent results.  $\sigma$ 's use Gaussian means and incorporate both errors. 74 Cf and 85 local control events were recorded (840 global control *i.e.* all of 2018).

Cf or AmBe, suggesting our novel detector, the “snowball chamber,” possesses ER “blindness” similar to PICO [5].

This would seem to contradict seminal work by [16] showing  $\gamma$  sensitivity, but even slightly different condi-

Calibration Type	$\langle \Delta t_{act} \rangle$ [s]	$\sigma$	$\langle T_{min} \rangle$ [°C]	$\sigma$
Ctrl (no source) '17	190.6 $\pm_{\pm 4.2}^{+2.8}$	-	-21.46 $\pm_{\pm 0.09}^{+0.07}$	-
AmBe Top no Pb	183.1 $\pm_{\pm 3.2}^{+3.5}$	-1.1	-21.85 $\pm_{\pm 0.39}^{+0.10}$	-0.9
AmBe Top yes Pb	150.5 $\pm_{\pm 17}^{+4.1}$	-2.2	-20.33 $\pm_{\pm 0.17}^{+0.13}$	4.7
$^{137}\text{Cs}$ $\gamma$ -ray Top	201.8 $\pm_{\pm 11}^{+3.6}$	0.9	-21.21 $\pm_{\pm 0.23}^{+0.12}$	0.9
Control 2018	149.5 $\pm_{\pm 7.6}^{+1.9}$	-	-19.63 $\pm_{\pm 0.19}^{+0.04}$	-
FWBe side (thin)	137.7 $\pm_{\pm 0.0}^{+16}$	-0.7	-19.71 $\pm_{\pm 0}^{+0.29}$	-0.2
FWBe side (thick)	124.6 $\pm_{\pm 9.9}^{+2.9}$	-1.9	-19.33 $\pm_{\pm 0.27}^{+0.07}$	0.9
AmBe side no Pb	158.9 $\pm_{\pm 23}^{+4.9}$	0.4	-19.96 $\pm_{\pm 0.44}^{+0.09}$	-0.7
AmBe Top no Pb	154.9 $\pm_{\pm 12}^{+3.8}$	0.4	-19.73 $\pm_{\pm 0.31}^{+0.09}$	-0.3
AmBe Top yes Pb	113.8 $\pm_{\pm 2.1}^{+4.4}$	-3.9	-18.88 $\pm_{\pm 0.01}^{+0.08}$	3.5
$^{252}\text{Cf}$ Top yes Pb	102.5 $\pm_{\pm 3.8}^{+4.0}$	-4.9	-18.46 $\pm_{\pm 0.22}^{+0.07}$	3.8

TABLE II. Means for the durations spent active ( $\Delta t_{act}$ ) by the water volume in all control and sources runs. Upper number is statistical error, lower number is systematic. The statistical significance (sigma) deviations from control (and directions) are included, using the total errors, assuming no correlations. Right half contains the lowest temperatures achieved prior to exothermic rise. The top 4 lines of the table, control through Cs, are for 2017, while the bottom are all for 2018. FWBe means Fiestaware, with different thicknesses of Be foil. Defaults were: source on top (except FWBe) and no Pb.

tions leading to different thresholds and nucleation probability may lead to a large increase in the ER rate (Appendix B). Also, the older observations were of needle-like tracks, not spheres as we observed, in Figure 4.

In contrast, the control and neutron results are significantly distinct, particularly for the  $^{252}\text{Cf}$  data set, with a difference of  $4.9\sigma$  for time and  $3.8\sigma$  for  $T$ , for the population averages. When Gaussian centroids are used instead, the discrepancies become 4.5 and 3.4 respectively (3.3 and 3.2 when comparing with “local” control only). As assuming Gaussianity and a particular binning can introduce biases, we also performed pairs of unbinned KS tests. The resulting p-values, for both time and  $T$ , were  $\ll 10^{-10}$  for comparison of Cf to all of the 2018 control. For local, the p’s are  $6.64 \times 10^{-5}$  and  $3.09 \times 10^{-8}$ , demonstrating Cf and control are not consistent statistically. Pair-wise checks of like with like (*i.e.* control or Cf with itself) indicated much greater consistency (p between 0.01-0.54). Individual event counts were: 26, 22, 32, 52, 27 (control, Cf, control, Cf, control respectively).

## B. Discussion

The  $^{252}\text{Cf}$  causing the water to be supercooled for less time than AmBe is sensible, as the source, while lower in energy, is  $\sim 15$ x stronger in neutron rate. The Cf was in fact selected due to its higher n-to- $\gamma$ -ratio compared to AmBe [13], and also to confirm a stronger source would produce a stronger effect, after seeing AmBe (2017) and FWBe results.

The effect of Pb is a mystery, however. While nearly all n sources cause higher  $T_{min}$  and lower times, they are not significant for AmBe without Pb. We can reject the hypothesis of  $\gamma$ ’s adversely affecting the thermocouples [17] as the rates were insufficient. We did find with G4 a 5% increase in NR rate in the presence of Pb, specifically for the oxygen (Appendix B) along with a general increase in average energy and  $dE/dx$  for O. We explored the possibility that the  $\gamma$ -rays from increased neutron captures on H were responsible for the effect we observe, but this is not likely, due to estimated  $dE/dx$  threshold. We were however unable to perform one more study, of  $^{252}\text{Cf}$  without Pb, due to equipment failure. Regardless, G4 indicates Pb is less impactful for Cf, versus AmBe.

It is unclear what the best models to use are for threshold and critical radius. After exploring many options, we were able to best fit our Cf data (pink in Fig. 5) using Figs. 2-4 of [19] following  $S_w = 0.97$  (related to pressure and geometry) resulting in the following equations:

- (1)  $E > E_c = 0.2 \text{ keV}$  (post eqs. 2-3  $E_c=1.2$  effectively)
- (2)  $dE/dx > E_c/r_c = 10 \text{ eV/nm} = 100 \text{ MeV/cm}$
- (3)  $l > 2r_c = 40 \text{ nm}$
- (4)  $Efficiency = 1/(1 + (T/252.8 \pm 1.1 \text{ K})^{540 \pm 150})$

where subscript  $c$  is critical. Eq. (3), ordinarily implied by (2), is necessary [14]: it ensures a particle traverses at minimum one critical diameter ( $l$  is track length). Otherwise, the proto-snowball may collapse. Applying these conditions to G4 results, all NR and ER below  $\sim 1$  keV are sub-threshold: see Appendix B, where we present the resulting  $dE/dx$  and energy spectra for recoiling species:  $e^-$ , H, O, with G4 cross-checked using NIST for the first two [22, 23]. Extreme degeneracy in fitting forced us to not float eqs. (1-3) above, so only a sigmoid efficiency for nucleation, unrelated to [19], was a free parameter, its steepness explaining reduced nucleation at  $T > -16$  °C.

Protons and  $e^-$ ’s fall below the critical  $dE/dx$  (*i.e.* threshold  $dE/dx$ ) but not O. This provides a plausible explanation for the lack of decreased supercooled time for Cs, which, despite all the shielding like steel flanges, still generated significantly more ER than other sources.

## V. CONCLUSION

This letter documents very strong initial evidence that MeV-scale neutrons can lead to supercooled water freezing. The feasibility of a full-scale water-based dark matter experiment is not established, not until we can lower thresholds, and increase live-time. The former should be quite feasible by going colder via greater purity [29–34].

One cannot pass over the many interdisciplinary implications. Studies of particles freezing supercooled water are highly germane to atmospheric sciences [35]. We may have resolved conflicting claims of radiation causing nucleation or not [25, 36]. The solution may be  $dE/dx$ . Our work also complements CLOUD at CERN [37]. Lastly, neutrons have been used to study the properties of supercooled water before [38–40] but not solidify it, as here.

## ACKNOWLEDGMENTS

This work was supported by the University at Albany, State University of New York (SUNY), under new faculty startup funding provided to Prof. Szydagis for 2014-18, and under the generous Presidential Innovation Fund for Research and Scholarship (PIFRS) grant awarded to Prof. Szydagis for 2017-18 by the Office of the Vice President for Research, Division of Research, the University at Albany, SUNY, as well as with a FRAP-A award (Faculty Research Award Program) and the startup funds of Prof. Levy. The research was partially supported by the Department of Energy under Award No. de-sc0015535,

allowing R&D part-time. We thank Dr. A. Bolotnikov of BNL for making us aware of previous work.

We also gratefully acknowledge the advice, encouragement, and support of the following individuals, who provided their knowledge plus expertise: our UAlbany colleagues Prof. Saj Alam and Prof. Bill Lanford. We thank Dr. Marc Bergevin of LLNL for an extraordinarily helpful discussion on the relative merits of AmBe / Cf sources. Lastly, Szydagis wishes to personally thank his wife Kel, a linguist not physicist by training, for suggesting the type of filter to use for purifying water and for coming up with the name of the snowball chamber.

- 
- [1] M. Battaglieri *et al.*, “US Cosmic Visions: New Ideas in Dark Matter 2017: Community Report,” in *U.S. Cosmic Visions: New Ideas in Dark Matter College Park, MD, USA, March 23-25, 2017*.
- [2] D. Akimov, J. B. Albert, P. An, C. Awe, P. S. Barbeau, B. Becker, V. Belov, A. Brown, A. Bolozdynya, B. Cabrera-Palmer, M. Cervantes, J. I. Collar, R. J. Cooper, R. L. Cooper, C. Cuesta, D. J. Dean, J. A. Detwiler, A. Eberhardt, Y. Efremenko, S. R. Elliott, E. M. Erkela, L. Fabris, M. Febbraro, N. E. Fields, W. Fox, Z. Fu, A. Galindo-Uribarri, M. P. Green, M. Hai, M. R. Heath, S. Hedges, D. Hornback, T. W. Hossbach, E. B. Iverson, L. J. Kaufman, S. Ki, S. R. Klein, A. Khromov, A. Konovalov, M. Kremer, A. Kumpan, C. Leadbetter, L. Li, W. Lu, K. Mann, D. M. Markoff, K. Miller, H. Moreno, P. E. Mueller, J. Newby, J. L. Orrell, C. T. Overman, D. S. Parno, S. Penttila, G. Perumpilly, H. Ray, J. Raybern, D. Reyna, G. C. Rich, D. Rimal, D. Rudik, K. Scholberg, B. J. Scholz, G. Sinev, W. M. Snow, V. Sosnovtsev, A. Shakirov, S. Suchyta, B. Suh, R. Tayloe, R. T. Thornton, I. Tolstukhin, J. Vanderwerp, R. L. Varner, C. J. Virtue, Z. Wan, J. Yoo, C.-H. Yu, A. Zawada, J. Zettlemoyer, A. M. Zderic, and , “Observation of coherent elastic neutrino-nucleus scattering,” *Science*, vol. 357, no. 6356, pp. 1123–1126, 2017.
- [3] S. Fukuda *et al.*, “The super-kamiokande detector,” *Nuclear Instruments and Methods in Physics Research Section A: Accelerators, Spectrometers, Detectors and Associated Equipment*, vol. 501, no. 2, pp. 418 – 462, 2003.
- [4] E. Behnke *et al.*, “First Dark Matter Search Results from a 4-kg CF<sub>3</sub>I Bubble Chamber Operated in a Deep Underground Site,” *Phys. Rev.*, vol. D86, no. 5, p. 052001, 2012. [Erratum: *Phys. Rev.*D90,no.7,079902(2014)].
- [5] C. Amole *et al.*, “Dark matter search results from the pico-60 c3f8 bubble chamber,” *Phys. Rev. Lett.*, vol. 118, p. 251301, Jun 2017.
- [6] V. Holten, J. V. Sengers, and M. A. Anisimov, “Equation of State for Supercooled Water at Pressures up to 400 MPa,” *Journal of Physical and Chemical Reference Data*, vol. 43, p. 043101, Dec. 2014.
- [7] L. W. Deitrich and T. J. Connolly, “A study of fission-fragment-induced nucleation of bubbles in superheated water,” *Nuclear Science and Engineering*, vol. 50, no. 3, pp. 273–282, 1973.
- [8] D. Barahona, “Thermodynamic derivation of the activation energy for ice nucleation,” *Atmospheric Chemistry & Physics*, vol. 15, pp. 13819–13831, Dec. 2015.
- [9] D. Barahona, “On the thermodynamic and kinetic aspects of immersion ice nucleation,” *Atmospheric Chemistry and Physics*, vol. 18, no. 23, pp. 17119–17141, 2018.
- [10] A. N. Nevzorov, “Some properties of metastable states of water,” *Phys. of Wave Phen.* 14(1), p. 4557, 2006.
- [11] E. Landa and T. Councell, “Leaching of Uranium from Glass and Ceramic Foodware and Decorative Items,” *Health Physics*, vol. 63, no. 3, pp. 343–348, 1992.
- [12] E. Aprile *et al.*, “Design and performance of the XENON10 dark matter experiment,” *Astroparticle Physics*, vol. 34, pp. 679–698, Apr. 2011.
- [13] C. E. Dahl, “The physics of background discrimination in liquid xenon, and first results from xenon10 in the hunt for wimp dark matter,” *PhD Thesis*, 2009.
- [14] M. Szydagis, “Dark matter limits from a 15 kg windowless bubble chamber,” *PhD Thesis*, 2011.
- [15] J. D. Atkinson, B. J. Murray, and D. OSullivan, “Rate of homogenous nucleation of ice in supercooled water,” *The Journal of Physical Chemistry A*, vol. 120, no. 33, pp. 6513–6520, 2016. PMID: 27410458.
- [16] N. C. Varshneya, “Detecting radiation with a supercooled liquid,” *Nature*, vol. 223, pp. 826–827, 08 1969.
- [17] G. J. Dau, R. R. Bourassa, and S. C. Keeton, “Nuclear radiation dose rate influence on thermocouple calibration,” *Nucl. Appl.*, vol. 5, no. 5, pp. 322–328, 1968.
- [18] E. Behnke *et al.*, “Direct measurement of the bubble-nucleation energy threshold in a cf<sub>3</sub>I bubble chamber,” *Phys. Rev. D*, vol. 88, p. 021101, Jul 2013.
- [19] V. Khvorostyanov and J. Curry, “The theory of ice nucleation by heterogeneous freezing of deliquescent mixed ccn. part i: Critical radius, energy, and nucleation rate,” *Journal of The Atmospheric Sciences - J ATMOS SCI*, vol. 61, pp. 2676–2691, 11 2004.
- [20] A. F. Pisarev, “On ion detection in supercooled liquids,” *CERN-Trans-67-7*, 1967.
- [21] F. Seitz, “On the Theory of the Bubble Chamber,” *Physics of Fluids*, vol. 1, pp. 2–13, Jan. 1958.
- [22] NIST, “<https://physics.nist.gov/PhysRefData/Star/Text/PSTAR.html>,” -, 2019.
- [23] NIST, “<https://physics.nist.gov/PhysRefData/Star/Text/ESTAR.html>,” -, 2019.
- [24] N. C. Varshneya, “On the principle of a radiation detector,” *Univ. Roorkee Res. J.*, vol. 8, 1 1965.
- [25] N. Varshneya, “Theory of radiation detection through supercooled liquid,” *Nuclear Instruments and Methods*,

- vol. 92, no. 1, pp. 147 – 150, 1971.
- [26] A. Pisarev, “new ideas of tracking cameras,” *Physics of Elementary Particles and Atomic Nuclei*, vol. v.3, no. p. n.3, pp. 650–687, 1972.
- [27] C. McCabe, “The Astrophysical Uncertainties Of Dark Matter Direct Detection Experiments,” *Phys. Rev.*, vol. D82, p. 023530, 2010.
- [28] E. Aprile *et al.*, “A Search for Light Dark Matter Interactions Enhanced by the Migdal effect or Bremsstrahlung in XENON1T,” *arXiv*, vol. 1907.11485, Sep 2019.
- [29] C. Goy *et al.*, “Shrinking of rapidly evaporating water microdroplets reveals their extreme supercooling,” *Phys. Rev. Lett.*, vol. 120, p. 015501, Jan 2018.
- [30] D. E. Hare and C. M. Sorensen, “The density of supercooled water. ii. bulk samples cooled to the homogeneous nucleation limit,” *The Journal of Chemical Physics*, vol. 87, no. 8, pp. 4840–4845, 1987.
- [31] N. E. Dorsey, “The freezing of supercooled water,” *Transactions of the American Philosophical Society*, vol. 38, no. 3, pp. 247–328, 1948.
- [32] E. K. Bigg, “The supercooling of water,” *Proc. of the Physical Society. Sec. B*, vol. 66, no. 8, p. 688, 1953.
- [33] S. C. Mossop, “The freezing of supercooled water,” *Proc. of the Phys. Soc. Sec. B*, vol. 68, no. 4, p. 193, 1955.
- [34] V. D. Aleksandrov, N. N. Golodenko, V. V. Dremov, V. A. Postnikov, O. V. Sobol’, M. V. Stasevich, and N. V. Shchebetovskaya, “Using numerical simulation methods for the analysis of heating and cooling thermograms characterizing the melting and crystallization of water,” *Technical Physics Letters*, vol. 35, pp. 415–417, May 2009.
- [35] F. Yu, “Formation of large nat particles and denitrification in polar stratosphere: possible role of cosmic rays and effect of solar activity,” *Atmospheric Chemistry and Physics*, vol. 4, no. 9/10, pp. 2273–2283, 2004.
- [36] L. H. Seeley, G. T. Seidler, and J. G. Dash, “Laboratory investigation of possible ice nucleation by ionizing radiation in pure water at tropospheric temperatures,” *Jrnl. Geo. Res.: Atmospheres*, vol. 106, pp. 3033–3036, 2001.
- [37] E. M. Dunne *et al.*, “Global atmospheric particle formation from cern cloud measurements,” *Science*, vol. 354, no. 6316, pp. 1119–1124, 2016.
- [38] R. Schiller and I. Kules, “Radiation chemistry of supercooled water,” *The Journal of Physical Chemistry*, vol. 75, no. 19, pp. 2997–2999, 1971.
- [39] A. Belitzky, E. Mishuk, D. Ehre, M. Lahav, and I. Lubomirsky, “Source of electrofreezing of supercooled water by polar crystals,” *Phys. Chem. Lett.*, vol. 7, 2015.
- [40] D. E. Hare and C. M. Sorensen, “Raman spectroscopic study of bulk water supercooled to 33c,” *The Journal of Chemical Physics*, vol. 93, no. 1, pp. 25–33, 1990.
-

## APPENDIX A: SUPPLEMENTARY EVIDENCE

This appendix contains additional analyses performed as cross-checks, given our claim of the first observation of a new physics/chemistry process, NR from neutrons freezing supercooled water, as well as the odd finding that only the lead-shielded n sources led to results of  $2 - 5\sigma$  significance. Below are all histograms for active time for all sources studied, with Gaussian fits. Mean values should be compared with Table II in the main text: all are quite similar.

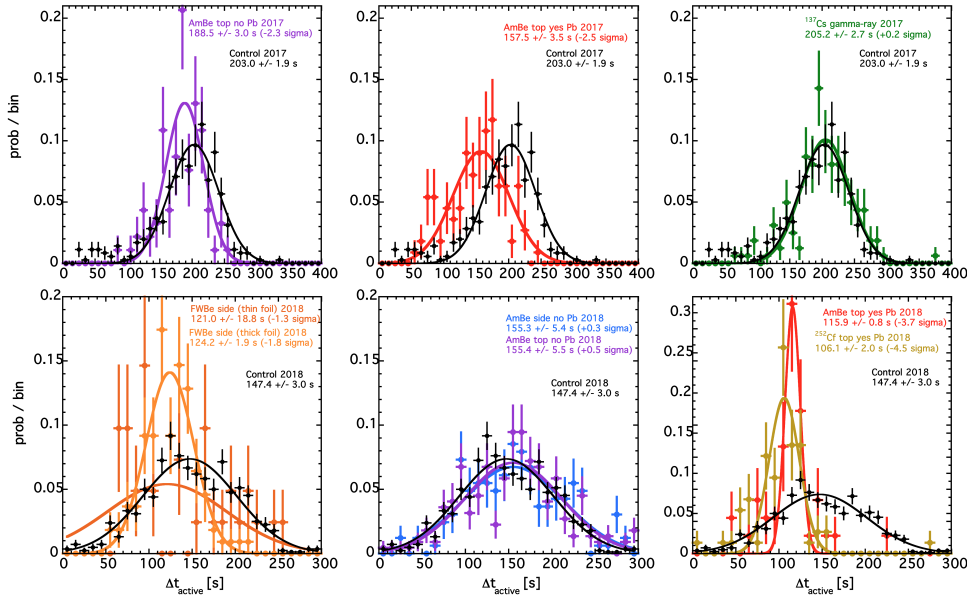


FIG. 6. The contrast with all of control for each source-on data set in terms of time spent active (*i.e.* sensitive) with the statistical significance in the legends. The top row consists of 2017 data, while the bottom is 2018, when brighter LEDs caused an overall decrease in time. Just the top thermocouple thermometer was always the reference, with exact value of temperature to use determined by checking for nucleation in the pre-trigger camera images. Note the marked difference for Cf, followed by AmBe with Pb the close second, while Cs is very consistent statistically with control.  $T_{\text{min}}$  plots, not pictured here, are similar. The systematic errors are not listed but included, from Table II.

Next, we contrast the different thermometers: top, middle, and bottom, for an example test case, of AmBe with Pb, the results from which were statistically significantly different from control, even though the no-Pb data were not, and the G4 sims showed only a small difference in (Oxygen) rate and recoil energy spectrum. The data are split up by year.

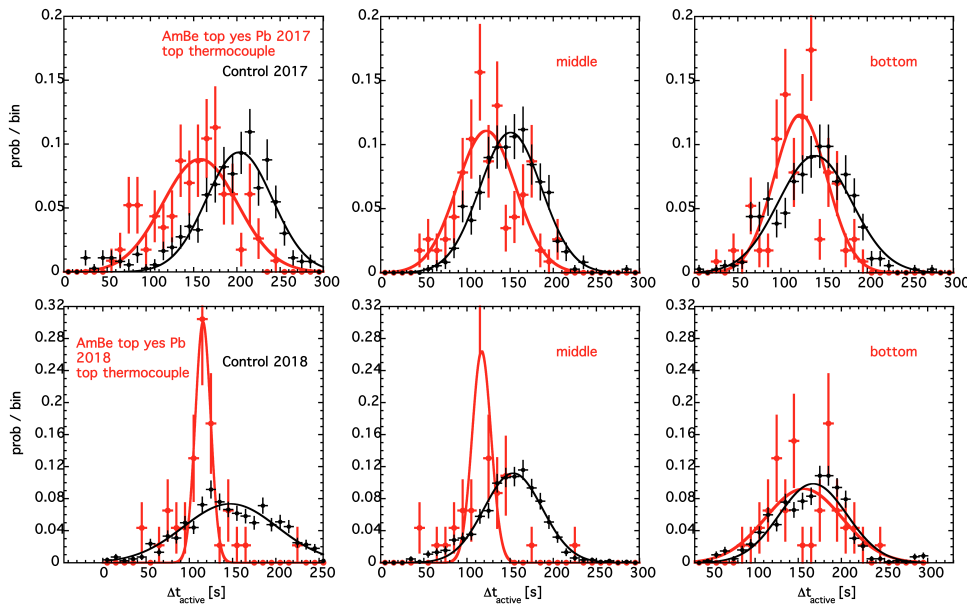


FIG. 7. 10s-bin-width histograms and Gaussian fits of time spent active, defined as below  $-16^\circ\text{C}$ , by AmBe (with Pb) in 2017 (top row) and 2018 (bottom row). The first column is the top thermometer, the standard in all the analyses reported in the paper, while the second and third columns are for the middle and bottom thermometers respectively. The control data are in black, and AmBe with Pb in red. Note the source-on distributions are always lower in time than for control, across all thermometers, even when not statistically significantly so. The top is also not always the most significant. The plots above and below are aligned such that it is possible to see that AmBe and control are markedly similarly distinct in their means, across the different setups separated by nearly a year.

## APPENDIX B: GEANT4 PLUS THRESHOLD SIMULATIONS

In this appendix greater detail is included for our G4 Monte Carlo, with the (critical) thresholds in energy,  $dE/dx$ , and track length applied on top of their results, along with a sigmoid-shaped efficiency for the NR-induced snowball nucleation. The work presented here was used to produce the pink curves in Fig. 5 in the main body of the text.

What we find in Table III is that the presence of the Pb shielding increased the NR interaction rate by 5% for AmBe, but made no significant change for Cf. Furthermore, the ER rate is two orders of magnitude higher for Cs than for the n sources, even when accounting for shielding and geometry. It is therefore extremely unlikely that gammas from the primarily-n sources can explain enhanced probability for nucleation in the presence of Cf and AmBe (with Pb). The Cf-induced NR rate exceeds AmBe by nearly twenty times, in keeping with the source strength difference.

GEANT Simulation	NR Rate [Hz]	ER Rate [Hz]
AmBe	0.155	$< 2 \times 10^{-4}$
AmBe w/ Pb	0.163	$< 2 \times 10^{-4}$
$^{252}\text{Cf}$	2.70	$< 8 \times 10^{-4}$
$^{252}\text{Cf}$ w/ Pb	2.70	$< 8 \times 10^{-4}$
$^{137}\text{Cs}$ gamma	0.000	$< 4 \times 10^{-2}$

TABLE III. The integrated rates above all thresholds for all sources and recoils, applying all three conditions for nucleation, including  $dE/dx > 100$  MeV/cm. Note that NR is strictly O. Upper limits on ER rates are based on simulation statistics: 5000, 5000, 1233, 1233, and 27.03 seconds of real-time simulated respectively by row. The Fiestaware (FW) plate is not included as its specifics were not well known, and results from it were not very significant. These rates allow us to reproduce and explain the data, in particular the Cf, at least after a fourth nucleation condition, of efficiency, is applied.

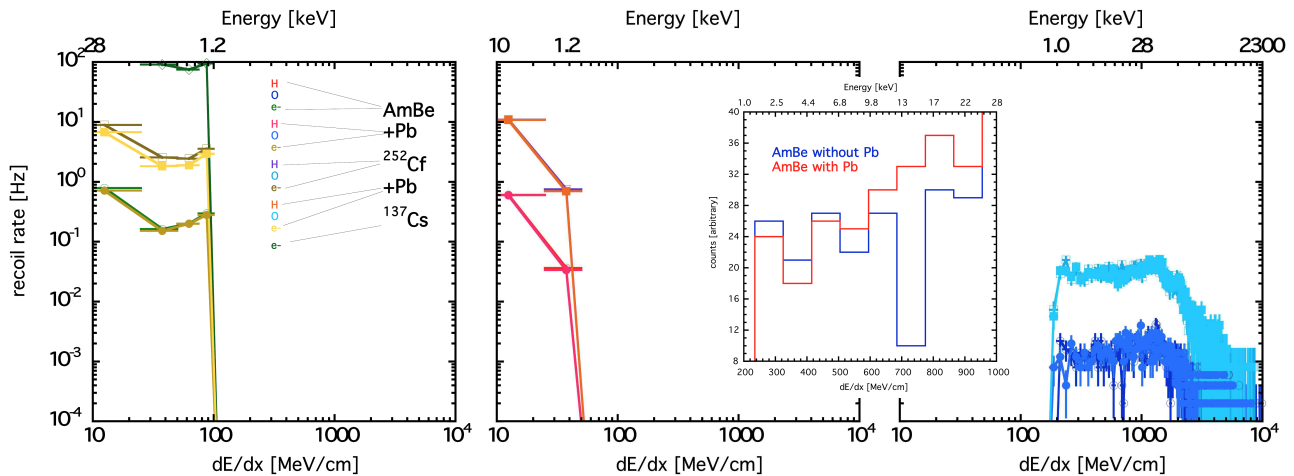


FIG. 8. The differential stopping power spectrum for each possible type of recoil in water, in the setup for this work, for sources tested (Cf without Pb, not studied, included for completeness). Corresponding initial species energies for which these are mean  $dE/dx$ 's are along the secondary, upper x-axes. The plot panes are, from left to right: electron, proton (hydrogen), and oxygen recoils, in shades of yellow, red, and blue respectively. A  $\sim 100$  MeV/cm threshold, a natural assumption, as explained in the text, explains the lack of discernible response from the  $\gamma$ -ray source (dark green diamonds and line near 100 Hz at upper left in first plot). The lines are not fits but visual guides, and errors are only bin widths (in x) or statistical (y). Integrated rates are in the earlier table (but AmBe top only not side included in both places due to similarity) *Inset* A break-down of O from right-most main plot, with no Pb data in red now, and with-Pb blue, and coarser binning. Note shift at 700 MeV/cm or 15 keV.

We can explain our apparent contradiction of earlier work, by Varshneya and Pisarev in [16, 20, 24–26] and references therein, documenting use of supercooled water to observe gammas and betas, but not neutrons, thus ER, not NR: the threshold energy is very sensitive to temperature and these previous works reporting data around  $-20$  °C do not always possess error bars. Only 1-2° colder could increase the ER rate from Cs for example from negligible to  $> 100$  Hz.

As to the feasibility of a dark matter experiment, even keV-scale not sub-keV threshold would be an improvement over current technologies, if coupled to light elements like O [27], particularly when combined with the ER discrimination presented here and corroborated by MC. While we have an apparent disadvantage with no visible proton recoils, on which was based hope for sensitivity to WIMPs of  $\leq 500$  MeV rest-mass energy, it is important to remember most ER backgrounds are minimally ionizing ( $\sim 2$  MeV/cm) so we can decrease  $dE/dx$  threshold safely, by lowering  $T$ .